

PAPER • OPEN ACCESS

## Effect of negative triangularity on tearing mode stability in tokamak plasmas

To cite this article: Xu Yang *et al* 2023 *Nucl. Fusion* **63** 066001

View the [article online](#) for updates and enhancements.

### You may also like

- [Pedestal properties of H-modes with negative triangularity using the EPED-CH model](#)  
A Merle, O Sauter and S Yu Medvedev
- [Zonal flow screening in negative triangularity tokamaks](#)  
Rameswar Singh and P.H. Diamond
- [To dee or not to dee: costs and benefits of altering the triangularity of a steady-state DEMO-like reactor](#)  
J.A. Schwartz, A.O. Nelson and E. Kolemen

# Effect of negative triangularity on tearing mode stability in tokamak plasmas

Xu Yang<sup>1,\*</sup>, Yueqiang Liu<sup>2</sup>, Wei Xu<sup>3</sup>, Yuling He<sup>4,\*</sup> and Guoliang Xia<sup>5</sup>

<sup>1</sup> Department of Physics, and Chongqing Key Laboratory of Intelligent Perception and BlockChain Technology, Chongqing Technology and Business University, Chongqing 400067, China

<sup>2</sup> General Atomics, PO Box 85608, San Diego, CA 92186-5608, United States of America

<sup>3</sup> National Research Base of Intelligent Manufacturing Service, Chongqing Technology and Business University, Chongqing 400067, China

<sup>4</sup> Guangdong Provincial Key Laboratory of Quantum Engineering and Quantum Materials, GPETR Center for Quantum Precision Measurement, SPTE, South China Normal University, Guangzhou 510006, China

<sup>5</sup> UKAEA, Culham Science Centre, Abingdon, OX14 3DB, United Kingdom of Great Britain and Northern Ireland

E-mail: [yangxu@ctbu.edu.cn](mailto:yangxu@ctbu.edu.cn) and [hey1@m.scnu.edu.cn](mailto:hey1@m.scnu.edu.cn)

Received 11 January 2023, revised 7 March 2023

Accepted for publication 24 March 2023

Published 11 April 2023



CrossMark

## Abstract

The influence of negative triangularity (NT) of the plasma shape on the  $n = 1$  ( $n$  is the toroidal mode number) tearing mode (TM) stability has been numerically investigated, with results compared to that of the positive triangularity (PT) counterpart. By matching the safety factor profile for a series of toroidal equilibria, several important plasma parameters, including the triangularity, the plasma equilibrium pressure, the plasma resistivity as well as the toroidal rotation, have been varied. The TM localized near the plasma edge is found to be more unstable in the NT plasmas as compared to the PT counterpart. The fundamental reason for this difference is the lack of favorable average curvature stabilization in NT configurations. Direct comparison of the Mercier index corroborates this conclusion. For the core-localized mode, where the difference in the local triangularity between NT and PT becomes small and the curvature stabilization is significantly reduced, larger Shafranov shift in the plasma core associated with the NT configuration results in more stable TM. The plasma toroidal flow generally stabilizes the TM in plasmas with both NTs and PTs. The flow stabilization is however weaker in the case of negative triangularity with finite plasma pressure.

Keywords: negative triangularity, tearing mode, toroidal flow

(Some figures may appear in colour only in the online journal)

## 1. Introduction

The tearing mode (TM) is one of the most important macroscopic magnetohydrodynamics (MHD) instabilities, that leads to reconnection of the magnetic field lines (near the location

of the instability) [1–3], degradation of the plasma energy confinement [4–6], and potentially plasma major disruption [7–9]. Large magnetic islands, induced by the TM or its neoclassical counterpart, limit the plasma equilibrium pressure in terms of the normalized values  $\beta = 2\mu_0 \langle P \rangle / B_0^2$  and  $\beta_N = \beta[\%]a[m]B_0[T]I_p[MA]$ , where  $\beta$  is the ratio of the volume averaged plasma pressure  $\langle P \rangle$  to the magnetic pressure,  $B_0$  the on-axis toroidal magnetic field strength,  $a$  the plasma minor radius and  $I_p$  the plasma total current.

It is well known that finite  $\beta$ , in association with the finite pressure gradient across the mode rational surface, stabilizes the TM via the favorable average curvature effect. This

\* Authors to whom any correspondence should be addressed.



Original content from this work may be used under the terms of the [Creative Commons Attribution 4.0 licence](https://creativecommons.org/licenses/by/4.0/). Any further distribution of this work must maintain attribution to the author(s) and the title of the work, journal citation and DOI.

so-called GGJ-effect [10] relies on the fact that, in a toroidal geometry, the average magnetic curvature favors mode stabilization in particular in ‘D’-shaped plasmas. The effect is captured by the resistive Mercier index  $D_R$ , which is typically negative in tokamak geometry. As interesting consequences, the GGJ-effect can introduce finite frequency to the mode even in a static plasma [11–13]. A rotating TM (in an initially static plasma) in turn generates net electromagnetic torque and drives plasma flow [12]. Furthermore, the GGJ-effect induced energy dissipation was also found responsible for a strong stabilization of the resistive-plasma resistive wall mode (RP-RWM) [12]. Finally, as  $\beta_N$  approaches the so-called no-wall Troyon limit, the plasma equilibrium pressure can be destabilizing to the TM, by coupling the instability to the ideal kink mode [12].

The boundary shape of the plasma poloidal cross-section plays important roles in the discharge performance in tokamak fusion devices [14–16]. Conventionally, a ‘D’-shaped plasma with positive triangularity (PT) has been shown to be favorable for reducing the energy transport and increasing the  $\beta_N$  limit [17, 18]. Recent experiments, however, have shown that a reversed ‘D’-shape with negative triangularity (NT) can also help reduce the turbulence-induced energy transport as well and reach a global confinement comparable to the H-mode regime of PT-plasmas [19–24]. In particular, significant experimental efforts have been devoted to studying plasmas with the NT shape, in TCV [22], DIII-D [23, 24], and recently in other devices as well. Absence of edge localized modes in NT-plasmas is another advantage. Because of the aforementioned (and other) interesting features associated with the NT-configuration, operation with reversed ‘D’-shape for the plasma boundary is becoming an attractive fusion concept during recent years [24–31].

The NT-configuration provides a possible solution to the divertor heat load issue. Nevertheless, the macroscopic stability in these plasmas needs more careful investigation. Earlier studies in [32] showed that plasmas with optimized pressure profiles can be stable to global kink modes with appropriate core pressure profile optimization. In this study, we investigate the effect of NT of the plasma shape on the tearing mode stability through modeling in toroidal geometry, and compare with that for the PT counterpart. Recent experiments in DIII-D with NT shape seem to produce discharges with benign TM activity [23]. But in general, evidence concerning the stability of the TM in NT plasmas, with respect to its PT-counterpart, is still inconclusive [21, 22]. This motivates our systematic numerical investigation in this work. The NT-effect on tearing mode has so far not been systematically investigated in theory and modeling, much less in terms of achieving physics understanding which is the primary focus of the present work. A recent study [31] has partially considered the NT-effect on the TM, but in the context of reversed magnetic shear plasma scenarios (i.e. on the so-called double tearing mode). Our results here reveal the key physics difference introduced by the NT-shape, as compared to the PT-shape, that affects the TM stability. More specifically, we find that the NT-shape substantially reduces the favorable average curvature stabilization, leading to a more robust TM instability in tokamak plasmas. As for

the toroidal modeling, we employ the MARS-F code [33] to solve the resistive MHD eigenvalue problem without ordering assumptions.

The paper is organized as follows. Section 2 describes a series of numerical plasma equilibria that we construct in full toroidal geometry, that covers plasma boundary shapes ranging from negative to PT. A key feature of these equilibria is that the safety factor profile is fixed to be nearly identical while varying the plasma triangularity. Section 3 reports detailed modeling results on the TM stability as well as discussions on the underlying physics effects associated with the GGJ-stabilization and the Shafranov shift. Section 4 summarizes the results.

## 2. Plasma equilibria

In this study, we adopt semi-analytic equilibria in toroidal tokamak geometry, without referencing to specific devices. These equilibria are constructed for physics understanding of the NT-shape on the TM stability, and appropriate constraints on the equilibria are employed to facilitate achieving the goal.

We consider lower single null divertor-like plasmas, with the boundary shape specified in the  $(R, Z)$  coordinates on the poloidal plane [34] and normalized by the plasma major radius  $R_0$  (which is assumed to be 3 m)

$$R(\theta) = 1 + \varepsilon \cos(\theta + \delta \sin(\theta)) \quad (2.1)$$

$$Z(\theta) = \varepsilon \kappa \sin(\theta) - b \exp \left[ - \left( \left| \theta + \frac{\pi}{2} \right| / c \right)^{3/2} \right] \quad (2.2)$$

where the parameters  $\varepsilon$ ,  $\delta$ ,  $\kappa$  define the inverse aspect ratio of the plasma, the triangularity and elongation of the plasma boundary shape. In order to construct a lower single null plasma configuration, we specify,  $b = 0.08$  and  $c = 0.5$ . The parameters  $\varepsilon$  and  $\kappa$  are fixed at 1/3 and 1.5, respectively, in this study. The key parameter that we vary is the boundary triangularity  $\delta$ . Figure 1(a) shows examples of the constructed plasma boundary shape while varying  $\delta$  from  $-0.3$  to  $0.3$ . As will be reported later, choosing this range of  $\delta$  well covers the physics regime (the GGJ-regime) of interest here—the GGJ-effect disappears when  $\delta < -0.3$  for the series of equilibria considered. We emphasize that the  $\delta$ -value here refers to that of the plasma boundary shape. In consistently computed equilibria as in our study, the triangularity varies inside the plasma, vanishing at the magnetic axis. In this study, we consider a parabolic equilibrium pressure profile  $P = P_0(1-s^2)$  shown in figure 1(b). Other types of pressure profiles have also been examined showing no qualitative modification to the final conclusion.

An important consideration in studying the TM is the safety factor profile  $q$ , which is known to strongly affect the mode stability via the radial location of the associated rational surfaces as well as the local magnetic shear. In order to eliminate the effect of the  $q$ -profile on the TM stability while scanning plasma triangularity, we tune the plasma current

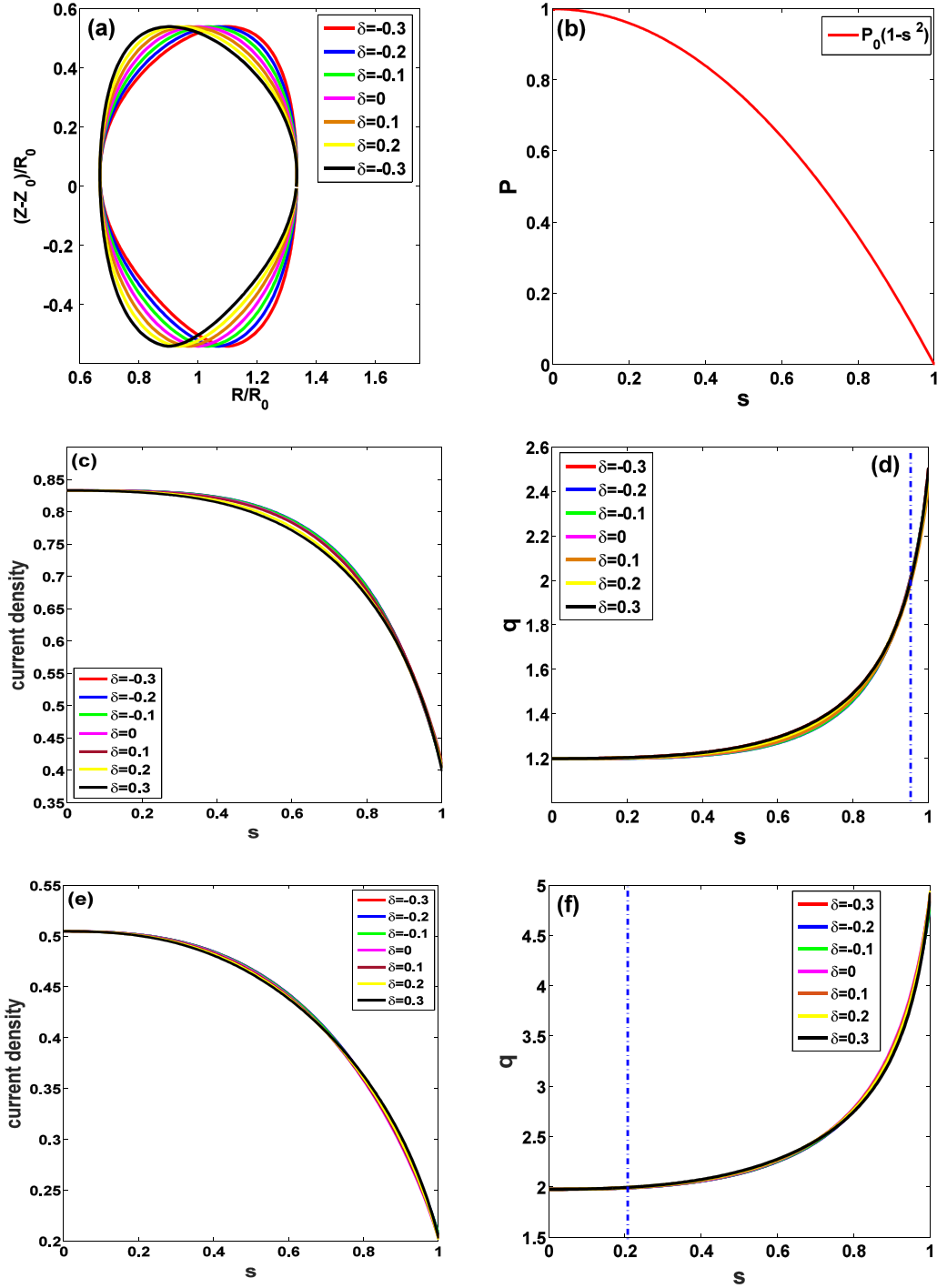


**Figure 1.** The (a) plasma boundary shapes (normalized by the major radius  $R_0$ ) with varying triangularity; (b) radial profiles of the pressure specified as  $P = P_0(1-s^2)$ ; (c), (e) radial profiles of the surface-averaged toroidal current density of the plasma; and (d), (f) radial profiles of the safety factor  $q$ , considered in this study. The vertical dash-dotted line in (d), (f) indicate the radial location of the  $q = 2$  rational surface.

density profile (which is one of the input data of our fixed-boundary equilibrium solver [35]) to ensure nearly identical safety factor profiles. Note that the safety factor is the output of the Grad-Shafranov solver here, and is numerically self-consistently computed. In this study, we utilize the CHEASE code [35, 36] for this purpose. The code takes the plasma boundary shape (e.g. figure 1(a)), the equilibrium pressure profile (figure 1(b)), and the surface-averaged toroidal current

density of the plasma (figures 1(c) and (e)) as input, then solves the fix-boundary Grad-Shafranov equation to obtain consistent numerical equilibria.

Two types of current density profiles (figures 1(c) and (e)) are considered, yielding two  $q$ -profiles (figures 1(d) and (f)). Figures 1(c) and (d) corresponds to one set of equilibria with  $q_0 = 1.2$  and  $q_{95} < 3$ . This is a case where the  $q = 2$  rational surface is located near the plasma edge (at  $s = 0.95$ ) where the

pressure gradient is also large. The triangularity values at the  $q = 2$  surface are  $-0.25, -0.18, -0.09, 0, 0.08, 0.18, 0.28$ . As a contrasting case (figures 1(e) and (f)), we construct a set of equilibria with  $q_0 = 1.98$  and  $q_{95} > 3$ . In this case, the  $q = 2$  rational surface is located near the plasma core (at  $s = 0.21$ ) where the pressure gradient is also small. The triangularity values at the  $q = 2$  surface are  $-0.07, -0.04, -0.03, 0, 0.03, 0.04, 0.05$  in this case. Note that to avoid the internal kink instability, we fixed the on-axis safety factor to be  $q_0 > 1$  for both cases.

### 3. Modeling results

We focus on investigating the effect of NT on the stability of the  $n = 1$  TM at the  $q = 2$  surface. Three plasma equilibrium parameters are of our primary concern while scanning the triangularity, i.e. the plasma pressure ( $\beta_N$ ), resistivity (Lundquist number  $S$ ), and the plasma toroidal rotation. We start by reporting the modeling results for plasmas with vanishing flow. In what follows (figures 2–5), we consider first the set of equilibria (with varying triangularity) described above with  $q_{95} < 3$ . This is the case where the contrast in the local (i.e. at the location of the TM) triangularity is more prominent.

Figures 2 and 3 report the MARS-F computed TM growth rate and mode frequency, respectively, for a series of equilibria with different triangularity while performing scans in 2D parameter space of  $\beta_N$  and  $S$ . The range for  $\beta_N$  is 0–1.77. The upper bound here is chosen to be reasonably below the Troyon no-wall limit for the onset of the  $n = 1$  ideal kink instability. At  $\beta_N > 1.77$ , we find that the TM eigenfunction becomes more global and starts to resemble that of an ideal kink. The range for the Lundquist number  $S$  is chosen to be  $2 \times 10^6 - 10^{10}$ . This covers the values for the Lundquist number in typical tokamak discharges. Note that the Lundquist number is defined as  $S = \tau_R/\tau_A$ , where  $\tau_R = \mu_0 a^2/\eta$  ( $\eta$  being the plasma resistivity and  $\mu_0$  vacuum permeability) is the resistive decay time of the plasma current and  $\tau_A = R_0 \sqrt{\mu_0 \rho_0}/B_0$  is the toroidal Alfvén time ( $R_0$  and  $a$  are the plasma major and minor radii, respectively).

Figure 2 shows that the TM growth rate generally decreases with increasing triangularity (from the negative to positive values). In fact with  $\delta \geq 0$  and sufficiently high Lundquist number ( $S \geq 10^8$ ), stable TM is computed in certain parameter spaces. At a given triangularity, the TM growth rate decreases with increasing Lundquist number. This is expected since the TM is driven by the plasma resistivity. It is on the other hand interesting to observe the different dependence of the mode stability on  $\beta_N$  between the NT- and PT-plasmas. For a NT-equilibrium (figures 2(a)–(c)), higher plasma pressure drives more unstable TM. The trend is however reversed for the PT-counterpart (figures 2(e) and (f)). The finite-pressure induced TM stabilization in PT-plasmas is associated with the GGJ-effect. The lack of such stabilization in the NT-plasmas indicates a weak GGJ-effect—an important finding of this study which will be further elaborated later on.

The presence of GGJ-stabilization often results in finite mode frequency (even in the absence of plasma rotation). This

is indeed the case for the PT-plasmas as shown in figure 3. As  $\delta$  is progressively increased from the negative to positive values, a region of finite-frequency appears in the  $(\beta_N, S)$  domain. This region emerges from the high- $S$  end for plasmas with weak NT (figures 3(c) and (d)), and becomes as a prominent feature for PT-plasmas (figures 3(e)–(h)). Presence of finite mode frequency is a clear indication of the GGJ-effect on the TM (at intermediate finite plasma pressure). Note that the regions with prominent frequency also correspond to the ‘meta-stable’ TM stability shown in figure 2. Absence of such regions for equilibria with strongly NT (figures 3(a) and (b)) indicates lack of GGJ-stabilization independent of the plasma pressure and resistivity.

As direct evidence for the presence or absence of the GGJ-effect, figures 4(a) and (b) shows the ideal ( $D_I$ ) and resistive ( $D_R$ ) Mercier indices evaluated at the  $q = 2$  surface, for the equilibria considered here. These equilibrium quantities are presented in the 2D parameter space of  $(\beta_N, \delta)$ . Note that  $D_I = 1/4$  corresponds to the case of vanishing plasma pressure where no GGJ-effect is present for all triangularity values. This quantity increases with both  $\beta_N$  and  $\delta$ . We mention that  $D_I$  exceeding unity corresponds to the ideal kink stability limit [37], which has evidently not been accessed for our series of equilibria.

The computed Mercier index  $D_R$  is of small negative values for the PT-plasmas at sufficiently high pressure (figure 4(b)). A negative  $D_R$  is directly associated with the GGJ-stabilization, which is proportional to  $D_R$  [10]. This quantity is however close to 0 for NT-equilibria, for a large range of  $\beta_N$  values. Figure 4(b) thus reveals the reason for the robust TM instability computed for the NT-plasmas as reported in figure 2.

Since the Shafranov shift is also known to affect the MHD instability, we evaluate this quantity as well for our equilibria, with results plotted in figure 4(c). Here, we define the Shafranov shift as the radial distance of the magnetic axis ( $R_{\text{axis}}$ ) with respect to the geometrical center ( $R_0$ ) of the plasma. The normalized quantity reported in figure 4(c) is thus  $\Delta/R_0 = (R_{\text{axis}} - R_0)/R_0$ . Figure 4(c) shows that the plasma pressure enhances the Shafranov shift, as expected. More importantly, increasing the plasma triangularity (from negative to positive values) results in reduced Shafranov shift. Since the Shafranov shift typically stabilizes MHD instabilities (in particular ballooning type of modes), the computed destabilization of the TM in the NT-plasmas (with large Shafranov shift) is not due to this effect. We thus conclude that the lack of the GGJ-stabilization is the main reason for the more unstable TM in NT-plasmas.

We have performed denser scan of the plasma triangularity than that reported in figures 2 and 3. Figure 5 show two representative examples of the computed TM growth rate versus  $\delta$ . One case ( $\beta_N = 0$  and  $S = 10^8$ ) is chosen from the top-left corner of the 2D parameter domain in figure 2, where the mode growth rate is too small to be clearly compared in the 2D plots. The other case ( $\beta_N = 0.5$  and  $S = 2 \times 10^6$ ) is chosen near the bottom-middle region from figure 2, where the instability remains relatively strong for all triangularity values. Note that we are also comparing two cases here with ( $\beta_N = 0.5$ ) and

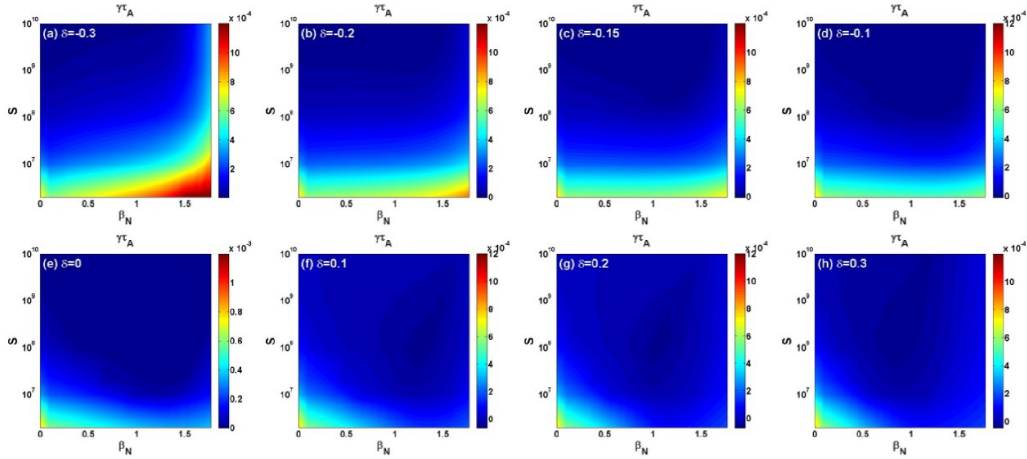


Figure 2. Plotted are the growth rate of the mode from negative to positive triangularity, while varying the  $\beta_N$  and the Lundquist number  $S$ .

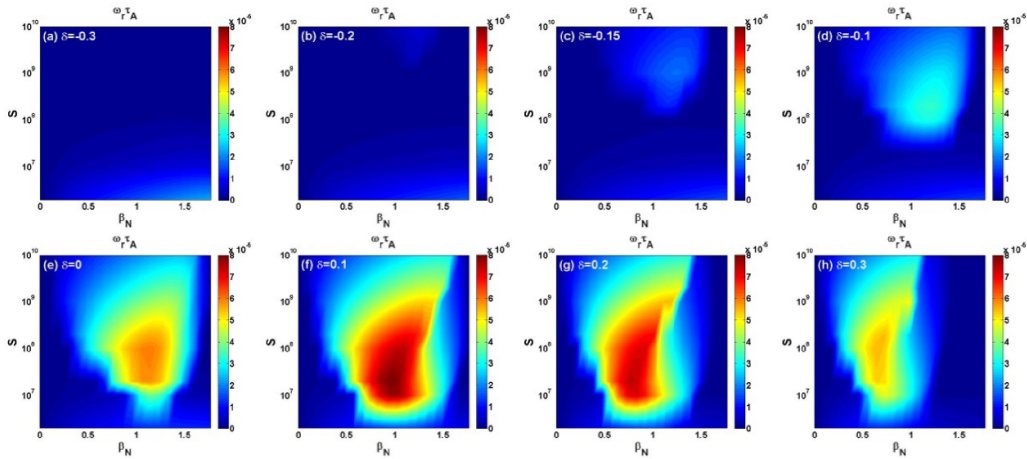


Figure 3. Plotted are the real frequency of the mode from negative to positive triangularity, while varying the  $\beta_N$  and the Lundquist number  $S$ .

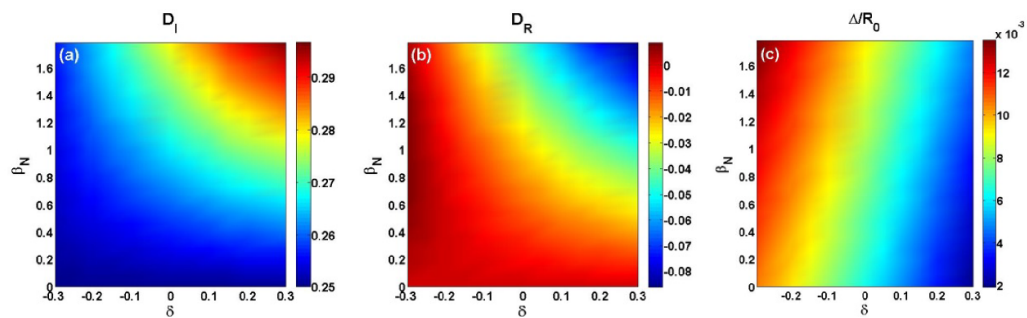
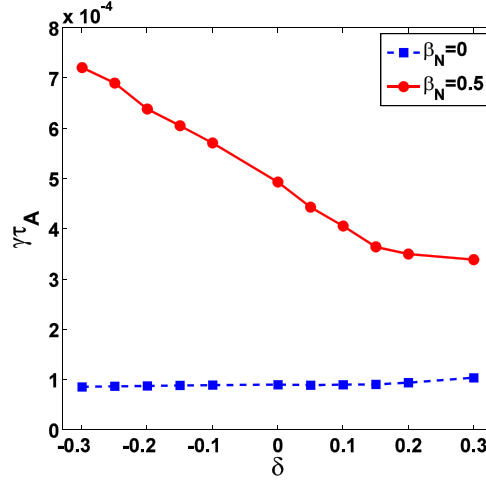


Figure 4. The (a) ideal and (b) resistive Mercier index at the  $q = 2$  surface, and (c) normalized Shafranov shift, while varying the  $\beta_N$  and the triangularity  $\delta$ .

without ( $\beta_N = 0$ ) the GGJ-effect. The presence of the favorable average curvature effect evidently results in substantial stabilization of the TM as we increase the plasma triangularity from negative to positive values. The slight stabilization (with decreasing  $\delta$ ) of the mode for the case of vanishing equilibrium pressure (thus no GGJ-stabilization) is related to the increase of the Shafranov shift as shown in figure 4(c).

We have so far systematically investigated stability of the TM located near the plasma edge. As mentioned earlier, this is motivated by the fact that the difference in the local triangularity (between the NT and PT configurations) is only prominent towards the plasma edge region. On the other hand, the Shafranov shift in the plasma core is significantly larger in NT plasmas (figure 4(c)). This can affect the stability of



**Figure 5.** The normalized growth rate of the  $n = 1$  tearing mode versus the plasma boundary triangularity  $\delta$ , computed assuming (a)  $\beta_N = 0$  and  $S = 10^8$ , and (b)  $\beta_N = 0.5$  and  $S = 2 \times 10^6$ .

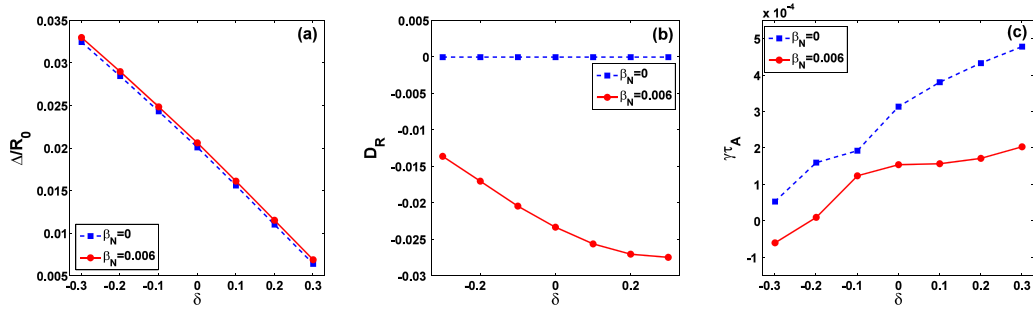


**Figure 6.** The (a) normalized Shafranov shift, (b) resistive Mercier index at the  $q = 2$  surface, and (c) growth rate of a core-localized  $n = 1$  tearing mode while varying the triangularity  $\delta$ , assuming  $S = 10^6$ . Compared are two cases with vanishing (blue dashed lines) and finite (red solid lines) equilibrium pressures. The equilibria correspond to the safety factor profiles shown in figure 1(f).

a core-localized TM despite of the vanishing difference in the local triangularity between the NT and PT configurations towards the magnetic axis. Because the Shafranov shift is stabilizing, we expect a more stable core-localized TM in the NT plasma, provided that the GGJ effect is sufficiently weak in both configurations (as it should be the case due to small equilibrium pressure gradient in the plasma core). The MARS-F computations (figure 6), utilizing the set of equilibrium profiles shown in figures 1(e) and (f), indeed confirm the above hypothesis.

Figure 6 show results of the (plasma surface) triangularity scan, while fixing the location of the  $q = 2$  surface at the minor radius of  $s = 0.21$ . Compared are two cases—one with vanishing equilibrium pressure (blue dashed lines) and the other with a finite but low pressure (red solid lines). In both cases, the TM is more stable towards the NT configuration (figure 6(c)). Note the strong increase of the core Shafranov shift NT plasmas (figure 6(a)), which stabilizes the TM. The more negative  $D_R$  values (and hence more GGJ stabilization, figure 6(b)) in the finite- $\beta_N$  case help stabilize the TM in PT plasmas, but this effect is somewhat weaker than that of the Shafranov shift stabilization. Further increasing  $\beta_N$  results in all equilibria being stable to the TM across our  $\delta$ -scan range.

As a final study of this work, we consider the NT effect on the TM stability in toroidally rotating plasmas. We again focus on the case with the mode located near the plasma edge. We consider two flow models, i.e. a uniform rotation along the plasma minor radius ( $\Omega = \Omega_0$ ) and a sheared rotation ( $\Omega = \Omega_0 (1 - s^2)$ ). The modeling results are reported in figure 7, again for the two cases of ( $\beta_N = 0$ ,  $S = 10^8$ ) and ( $\beta_N = 0.5$ ,  $S = 2 \times 10^6$ ) as in figure 7. Note that, with the same on-axis rotation frequency  $\Omega_0$ , the plasma rotation at the  $q = 2$  rational surface is much slower for the sheared flow case, as compared to the uniform flow. This motivates our choice of larger ranges for  $\Omega_0$  for sheared flow cases, in particular for the case with finite equilibrium pressure as shown in figures 7(d) and (h).

In general, we find that the plasma toroidal rotation reduces the TM growth rate independent of the flow models. For the  $\beta_N = 0$  case (figures 7(a) and (b)), the degree of stabilization is similar between NT- and PT-plasmas. At finite equilibrium pressure (figures 7(c) and (d)), however, the TM growth rate is less affected by plasma rotation for NT-equilibria. In all cases, the mode frequency roughly linearly increases with the plasma local rotation frequency at the  $q = 2$  surface (figures 7(e)–(h)), as expected.

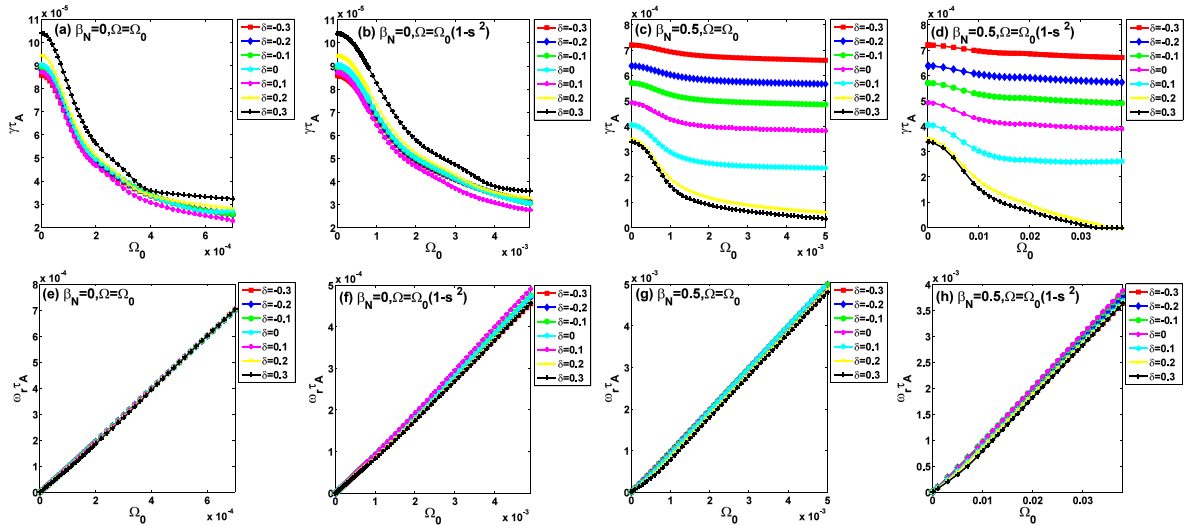


**Figure 7.** The computed normalized (a)–(d) growth rate, and (e)–(h) real frequency of the  $n = 1$  tearing mode, assuming ((a), (b), (e), (f))  $\beta_N = 0$  and  $S = 10^8$ , and ((c), (d), (g), (h))  $\beta_N = 0.5$  and  $S = 2 \times 10^6$ , while varying the plasma toroidal rotation frequency. Assumed are two rotation profile models, with ((a), (c), (e), (g)) a uniform rotation profile  $\Omega = \Omega_0$  along the plasma minor radius and ((b), (d), (f), (h)) a sheared rotation profile  $\Omega = \Omega_0(1 - s^2)$ .

#### 4. Conclusion and discussion

We have numerically investigated the influence of (negative) plasma triangularity on the  $n = 1$  TM in this work. By matching the safety factor profile for a series of toroidal equilibria, we scan several plasma parameters including the triangularity, the plasma equilibrium pressure, the plasma resistivity as well as the toroidal rotation.

For the TM located near the plasma edge, where the local triangularity differs the most between the NT and PT configurations, the instability is found to be more unstable in NT-plasmas as compared to the PT-counterpart. The fundamental reason for this difference is the lack of favorable average curvature stabilization in NT-plasmas, at least for the TM. (We point out that this lack of curvature stabilization also applies to other instabilities such as the ballooning-type of modes in NT plasmas.) Comparison of the Mercier index corroborates this conclusion. The Shafranov shift, which tends to be larger for the NT-equilibria, does not help to stabilize the mode except for the peculiar case of vanishing equilibrium pressure.

On the other hand, the core-localized TM is found to be more stable in the NT configuration. This is primarily due to the much stronger Shafranov shift in the plasma core in NT plasmas, as compared to the PT counterpart. The GGJ-effect is generally weaker in both NT and PT plasmas due to smaller equilibrium pressure gradient in the plasma core. These numerical findings clearly illustrate the two competing effects—the Shafranov shift and the GGJ-effect—for the TM stabilization as long as the plasma triangularity is concerned. The radial location of the mode plays an important role in determining whether the (negative) triangularity is stabilizing or destabilizing.

The plasma toroidal flow generally stabilizes the TM in plasmas with both NTs and PTs. For the cases of vanishing equilibrium pressure, the degree of stabilization is similar

between the NT- and PT-plasmas. For finite pressure cases, however, we find that the flow stabilization is weaker for the NT-plasma.

The above findings, in particular the physics understanding revealed by the numerical modeling, can be useful for interpreting experimental results in NT-plasmas. On the other hand, we point out that not all physics effects have been included in our present study, such as the neoclassical effects (NTM) and the non-linear effects, effects beyond standard single-fluid MHD model (e.g. anisotropic thermal transport effect which we will study in the near future). Some of these effects may also significantly affect the TM behavior in negative-triangularity plasmas.

#### Acknowledgments

This work was supported by the National Natural Science Foundation of China (Grant Nos. 11905022 and 11905067), China Postdoctoral Science Foundation under Grant No. 2022M711221, Chongqing Basic Research and Frontier Exploration Project in 2019 (Chongqing Natural Science Foundation, Grant No. cstc2019jcyj-msxmX0567), the Science and Technology Research Program of Chongqing Municipal Education Commission (Grant No. KJQN202200819), the project of Chongqing Technology and Business University (Grant Nos. 1952039 and 2056017), and Guangzhou Basic and Applied Basic Research Project under Grant No. 202201010619. This work was part-funded by the EPSRC Energy Programme (Grant No. EP/W006839/1). The work was also supported by the U.S. DoE Office of Science under Contract Nos. DE-FG02-95ER54309 and DE-FC02-04ER54698. This report was prepared as an account of work sponsored by an agency of the United States Government. Neither the United States Government nor any agency thereof,



nor any of their employees, makes any warranty, express or implied, or assumes any legal liability or responsibility for the accuracy, completeness, or usefulness of any information, apparatus, product, or process disclosed, or represents that its use would not infringe privately owned rights. Reference herein to any specific commercial product, process, or service by trade name, trademark, manufacturer, or otherwise, does not necessarily constitute or imply its endorsement, recommendation, or favoring by the United States Government or any agency thereof. The views and opinions of authors expressed herein do not necessarily state or reflect those of the United States Government or any agency thereof.

## ORCID iDs

Yueqiang Liu  <https://orcid.org/0000-0002-8192-8411>

Yuling He  <https://orcid.org/0000-0002-9765-227X>

## References

- [1] Furth H.P., Killeen J. and Rosenbluth M.N. 1963 *Phys. Fluids* **6** 459–84
- [2] Chu M.S., La Haye R.J., Austin M.E., Lao L.L., Lazarus E.A., Pletzer A., Ren C., Strait E.J., Taylor T.S. and Waelbroeck F.L. 2002 *Phys. Plasmas* **9** 4584
- [3] Huang W. and Zhu P. 2021 *Nucl. Fusion* **61** 036047
- [4] Nishimura Y. and Azumi M. 1997 *Phys. Plasmas* **4** 2365
- [5] La Haye R.J. 2006 *Phys. Plasmas* **13** 055501
- [6] Hu Q., Du X., Yu Q., Logan N.C., Kolemen E., Nazikian R. and Jiang Z.H. 2019 *Nucl. Fusion* **59** 016005
- [7] Kikuchi M. and Azumi M. 2012 *Rev. Mod. Phys.* **84** 1807–54
- [8] Wei L., Wang Z.-X., Wang J. and Yang X. 2016 *Nucl. Fusion* **56** 106015
- [9] Huang W. 2022 *Plasma Phys. Control. Fusion* **64** 055023
- [10] Glasser A.H., Greene J.M. and Johnson J.L. 1976 *Phys. Fluids* **19** 567
- [11] Liu Y., Connor J.W., Cowley S.C., Ham C.J., Hastie R.J. and Hender T.C. 2012 *Phys. Plasmas* **19** 072509
- [12] Hao G.Z., Liu Y.Q., Wang A.K., Xu M., Qu H.P., Peng X.D., Wang Z.H., Xu J.Q. and Qiu X.M. 2014 *Phys. Plasmas* **21** 012503
- [13] Liu T., Yang J.F., Hao G.Z., Liu Y.Q., Wang Z.X., Zheng S., Wang A.K. and He H.D. 2017 *Plasma Phys. Control. Fusion* **59** 065009
- [14] Moret J.M. *et al* 1997 *Phys. Rev. Lett.* **79** 2057
- [15] Fontana M., Porte L., Coda S. and Sauter O. 2018 *Nucl. Fusion* **58** 024002
- [16] Yang X., Liu Y., Xu W., He Y. and Lu S. 2022 *Nucl. Fusion* **62** 016013
- [17] Yamazaki K. 1980 *Jpn. J. Appl. Phys.* **19** 963
- [18] Wilson H.R., Snyder P.B., Huysmans G.T.A. and Miller R.L. 2002 *Phys. Plasmas* **9** 1277
- [19] Camenen Y., Pochelon A., Behn R., Bottino A., Bortolon A., Coda S., Karpushov A., Sauter O., Zhuang G. and Team T.T. 2007 *Nucl. Fusion* **47** 510–6
- [20] Kirneva N.A. *et al* 2012 *Plasma Phys. Control. Fusion* **54** 015011
- [21] Marinoni A., Sauter O. and Coda S. 2021 *Rev. Mod. Plasma Phys.* **5** 6
- [22] Weisen H. *et al* 1997 *Nucl. Fusion* **37** 1741
- [23] Marinoni A. *et al* 2021 *Nucl. Fusion* **61** 116010
- [24] Austin M.E. *et al* 2019 *Phys. Rev. Lett.* **122** 115001
- [25] Sauter O. *et al* 2014 *Phys. Plasmas* **21** 055906
- [26] Ren J., Liu Y., Liu Y., Medvedev S.Y., Wang Z. and Xia G. 2016 *Plasma Phys. Control. Fusion* **58** 115009
- [27] Ren J., Liu Y., Liu Y. and Medvedev S.Y. 2018 *Nucl. Fusion* **58** 126017
- [28] Xue L., Zheng G.Y., Duan X.R., Liu Y.Q., Hoang G.T., Li J.X., Dokuka V.N., Lukash V.E. and Khayrutdinov R.R. 2019 *Fusion Eng. Des.* **143** 48–58
- [29] Zhou L., Liu Y., Siccino M., Fable E., Wu T., Kurki-Suonio T., Varje J. and Liu D. 2021 *Plasma Phys. Control. Fusion* **63** 065007
- [30] Abate D., Marchiori G., Bettini P. and Villone F. 2020 *Plasma Phys. Control. Fusion* **62** 085001
- [31] Wang H.Y., Liu T., Liu Y.Q. and Wang Z.X. 2022 *Plasma Phys. Control. Fusion* **64** 085005
- [32] Medvedev S.Y. *et al* 2015 *Nucl. Fusion* **55** 063013
- [33] Liu Y.Q., Bondeson A., Fransson C.M., Lennartson B. and Breitholtz C. 2000 *Phys. Plasmas* **7** 3681–90
- [34] Liu Y., Lao L., Li L. and Turnbull A.D. 2020 *Plasma Phys. Control. Fusion* **62** 045001
- [35] Lütjens H., Bondeson A. and Roy A. 1992 *Comput. Phys. Commun.* **69** 287–98
- [36] Lütjens H., Bondeson A. and Sauter O. 1996 *Comput. Phys. Commun.* **97** 216
- [37] Brennan D.P., Strait E.J., Turnbull A.D., Chu M.S., La Haye R.J., Luce T.C., Taylor T.S., Kruger S. and Pletzer A. 2002 *Phys. Plasmas* **9** 2998